

Chimia 55 (2001) 861–866
© Schweizerische Chemische Gesellschaft
ISSN 0009–4293

Electrostatic Interactions in Biomolecular Systems

Philippe H. Hünenberger*, Ulf Börjesson, Roberto D. Lins

Abstract: Electrostatic interactions are of fundamental importance in determining the structure, dynamics, and function of biomolecules. In particular, they play a key role in protein folding and stability, pH-induced conformational changes, recognition of substrates by receptors, enzymatic catalysis, and in the formation of polysaccharide-based gels. However, due to their magnitude and long-range nature, the accurate representation of electrostatic interactions in classical computer simulations is a difficult task. There is thus considerable effort in the scientific community towards the goals of (i) improving the representation of electrostatic interactions in biomolecular simulations, and (ii) understanding their specific role in biomolecular processes. The present article reviews some of the work carried out in our group along these two lines.

Keywords: Acid-base properties · Carbohydrate simulation · Computer simulation · Electrostatic interactions · Protein stability

Introduction

From the point of view of quantum mechanics, chemistry can be described as the science of electrostatic interactions (between nuclei and electrons). However, to reach system sizes and timescales compatible with the experimental world, many (bio-)molecular simulations rely on a classical description of molecular systems [1]. In this case, specific types of electronic effects (covalent, exchange-repulsion, dispersion, and long-range electrostatic interactions) are grouped into the different terms of a force field (potential energy function), and classical electrostatic interactions only encompass the long-range residual of quantum electrostatics. This long-range tail is usually represented by the Coulombic interaction between atomic partial charges located on the solute and solvent molecules. Due to their magnitude and long-range nature, the accurate representation of long-range electrostatic interactions in classical computer simulations is a difficult task, and an area of on-going research [2–5]. This problem is particularly important be-

cause electrostatic interactions play a fundamental role in numerous processes of biochemical interest (*e.g.* protein folding, pH-induced conformational changes, molecular recognition, formation of gels, *etc.*). The present article gives a brief account of the work carried out in our group towards the goal of better representing and understanding electrostatic interactions in biomolecular systems.

Treatment of Electrostatic Interactions in Molecular Simulations

The approximate treatment of electrostatic interactions in computer simulations of explicit-solvent (bio-)molecular systems currently represents one of the bottlenecks in the accuracy of these methods [2–5]. This is because, due to computational costs, simulated systems are restricted to very small sizes (typically about 500–1000 nm³). As a direct consequence, the longest-range (4–5 nm) component of intermolecular interactions can only be computed in an approximate manner. However, due to the magnitude and long-range nature of electrostatic interactions, uncontrolled approximations can give rise to important artifacts (so-called finite-size effects), which may strongly impair the reliability of many current simulations.

The majority of explicit-solvent biomolecular simulations are carried out under periodic boundary conditions. In this case, the solute biomolecule is placed into a computational box (space-filling shape, *e.g.* rectangular parallelepiped), and the empty volume filled by solvent molecules. The system considered in the simulation consists of the central box surrounded by an infinite array of periodic copies of itself [2][6], which has the advantage of removing any distortion associated with a solvent/vacuum boundary. There are essentially three methods to handle electrostatic interactions in simulations under periodic boundary conditions. Straight truncation (ST) of the Coulomb interaction at a convenient (cutoff) distance [2][6], in order to limit the computational costs and the effect of periodic boundary conditions, is often a very severe approximation, leading to important artifacts in many simulated properties [7–13]. Two alternative schemes are available to reduce these effects: the inclusion of a reaction-field (RF) correction [14][15] to the cutoff truncation, or the use of lattice-sum (LS) methods (Ewald [16], P³M [17], PME [18]). These two types of methods also involve approximations, although presumably less drastic than the straight truncation of the long-range interactions. It is therefore of importance to carefully investigate and compare the accuracy

*Correspondence: Prof. P.H. Hünenberger
Department of Chemistry
Swiss Federal Institute of Technology
ETH Hönggerberg
CH-8093 Zürich
Tel.: +41 1 632 55 03
Fax: +41 1 632 10 39
E-Mail: phil@igc.phys.chem.ethz.ch

of these different methods. Our strategy to analyze and improve electrostatic schemes for explicit-solvent molecular simulations is to use continuum electrostatics, with the goal of understanding, correcting, and ultimately eliminating finite-size effects [5][12][13][19][20].

Simulations of biomolecular systems (and in particular DNA, RNA, and proteins) using LS methods are beginning to abound in the literature. LS methods are formally exact for truly periodic systems (crystals), but only approximate for the simulation of real (non-periodic) solutions [5]. However, little work has been done to assess the nature and magnitude of the perturbation that arises from artificial periodicity. Our approach to study this perturbation based on continuum electrostatics is the following. The reaction potential (and solvation free energy) generated by the solvent around a solute of arbitrary shape and charge distribution can be determined by solving the Poisson equation using a finite-difference scheme [21]. This can be done both for non-periodic boundary conditions [21] and for periodic boundary conditions [13]. By comparing the two results, the effect of the artificially imposed periodicity on the solvation free energy of a (bio-)molecule (in a given conformation) can be assessed quantitatively [5][13][19][20]. In cases where this perturbation is small (large computational box, solvent of high permittivity, solute with no net charge and of low polarity), the explicit-solvent simulation of the system using LS methods will be a reasonable approximation to the non-periodic case (macroscopic sample at infinite dilution). In other cases, the continuum method may be used to compute corrections for the finite-size effects affecting the simulated properties.

Continuum electrostatics methods can also be used to investigate finite-size effects linked with the ST and RF schemes, as well as some others (shifting and switching functions [2]). Although artifacts linked with the ST scheme are very important [7–13], the RF method appears to be a viable alternative to LS methods for the simulation of biomolecular systems, and is also used by many research groups. As a first step in the continuum electrostatics analysis of the ST, RF and related schemes, we considered the solvation of a spherical ion [12]. A generalized Born model was developed, where the r^{-1} -dependence of Coulomb's law is replaced by an arbitrary polynomial, truncated at the cutoff distance. It was possible to derive an analytical integral equation defining the polarization around

the ion, and thus allowing the computation of the ionic solvation free energy. This model was used to assess the quality of different approximations employed in explicit-solvent simulations, and derive corrections to ionic solvation free-energies calculated from these simulations [12]. It is also known from explicit-solvent simulations that cutoff truncation strongly affects the effective interaction (potential of mean force) between two solvated ions. Due to finite-size artifacts, this effective interaction may even become attractive over a certain range of distance for two ions of the same charge [10]. To tackle this problem, we are currently constructing a continuum electrostatics model describing the interaction between two spherical ions in the presence of cutoff truncation (ST or RF). An alternative route is the use of a newly developed algorithm for solving the Poisson equation for a solute-solvent system under periodic boundary conditions using fast Fourier transforms [22]. This method may easily be extended to truncated Coulomb interactions, which should permit a systematic analysis (and possibly correction) of cutoff-linked finite-size effects in complex molecular systems.

Two prototypical examples illustrate that the above considerations are far from academic. The first example is the calculation of ionic solvation free energies.

Values computed from molecular dynamics simulations of the sodium cation (parameters from Straatsma & Berendsen [8]) range from -250 to -460 kJ/mol [23], depending on the electrostatic scheme employed (LS, ST, or RF) and parameters used (edge of the cubic box in the range 1.2–4 nm, cutoff radius in the range 0.8–1.4 nm). However, when appropriate corrections for finite-size effects based on continuum electrostatics are applied, all results converge to an estimate of -399 ± 2 kJ/mol, in reasonable agreement with the experimental value of -370 kJ/mol.

The second example illustrates the influence of artificial periodicity on the conformational equilibrium of a polyalanine octapeptide (with charged termini) in water. Three explicit-solvent molecular dynamics simulations of this peptide were compared, using a LS method (P³M [17]) for handling electrostatic interactions together with cubic periodic boxes of edges $L=2, 3,$ and 4 nm [20]. The α -helix was found to be stable and rigid in the smallest box, stable but less rigid in the medium box, and unfolding in the largest box (see Fig. 1). Only the latter behavior agrees with experiment. The observed differences could be rationalized using a continuum electrostatics analysis of periodicity-induced artifacts (see above) based on configurations from the trajectories. These calculations show

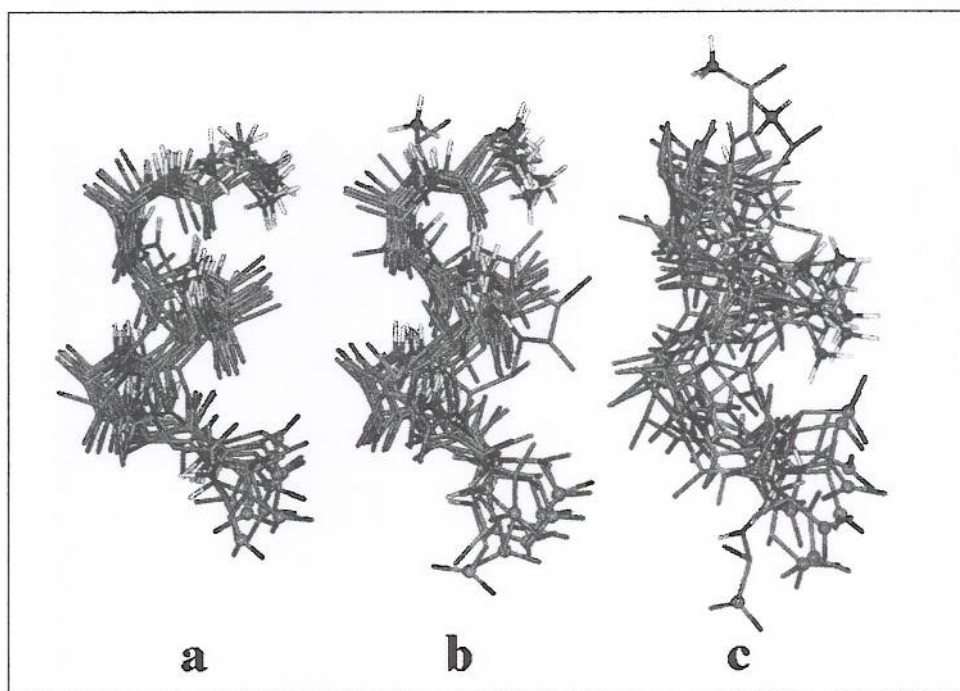


Fig. 1. Ten configurations (superimposed on the C_{α} atoms) taken at 0.1 ns intervals from three explicit-solvent molecular dynamics simulations [20] of a polyalanine octapeptide (charged termini) at 300 K, initiated from the α -helical conformation (distance from the ammonium nitrogen to the carboxylate carbon: 1.27 nm). The three simulations were carried out using lattice-sum electrostatics (P³M [17]) and employed cubic computational boxes of edges (a) $L=2$ nm, (b) $L=3$ nm, and (c) $L=4$ nm, containing 234, 866 and 2099 water molecules, respectively.

that the α -helical conformation is stabilized by artificial periodicity relative to any other configuration sampled during the simulations. This stabilization is due to the favorable interaction between the charged termini of the oligopeptide in the central computational box and those of its periodic copies in the adjacent boxes. This artifact increases in magnitude with decreasing box size, and is responsible for the absence of unfolding in the two smaller boxes and the reduced backbone fluctuations in the smallest box.

These results suggest that electrostatic finite-size effects in explicit-solvent simulations of biomolecules may significantly perturb the potentials of mean force for conformational equilibria. The effect may be so strong as to invert the relative stabilities of the folded and unfolded states of a peptide [20]. Because of the potential implications of these findings for the reliability of many biomolecular simulations, we are currently performing a systematic study of finite-size effects in simulations of complex biomolecular systems, including an oligonucleotide (double-stranded DNA dodecamer), a small charged protein (insulin gene enhancer protein ISL-1), and a membrane patch (2x64 dipalmitoylphosphatidylcholine double layer), with different electrostatic schemes (SC, RF, or LS), parameters (cutoff distance, box size), and numbers of counter-ions (none, minimal set, or excess).

Molecular Dynamics Simulation at Constant pH

The pH is one of the fundamental characteristics of aqueous solutions, and exerts a strong influence on the physico-chemical properties of solvated (bio-)molecules. For example, besides temperature, pressure, ionic strength, and the possible presence of denaturing agents, the pH is one of the major factors determining the structure of proteins in solution [24][25]. Although efficient algorithms have been developed for performing molecular dynamics simulations at constant temperature (thermostat) and pressure (manostat) [2][26], the effect of the pH is usually treated in a very primitive way in current molecular simulations: depending on the selected pH and on the approximate pK_a of a given ionizable group, either the protonated or the unprotonated state is selected and used for the whole simulation. When applied to large polyfunctional (bio-)molecules, this simplistic approach neglects impor-

tant effects: (i) the influence of the local environment (and its fluctuation in time) on the protonation state of a group; (ii) the influence of the protonation states of the ionizable groups (and their fluctuations in time) on the conformation of the molecule; (iii) the correlation between the protonation states of different groups. A proper representation of the three above effects in molecular simulations can only be achieved if the protonation states of the ionizable groups are treated as variables. Based on this approach, we are developing a new methodology for performing simulations of molecular systems at constant pH, *i.e.* an acidostat algorithm [27].

In our approach, each ionizable (titratable) group is treated as a mixed state, *i.e.* the interaction-function parameters for the group are a linear combination of those of the protonated state and those of the deprotonated state, in proportions determined for each group i by a coupling parameter λ_i . Free protons are not handled explicitly. Instead, the extent of deprotonation λ_i of each group is allowed to fluctuate in time, depending on the instantaneous system configuration and the imposed pH. The value of each λ_i variable is relaxed towards its equilibrium value λ_i^0 by weak-coupling [26] to a 'proton bath'. The target value λ_i^0 is determined for each group on the basis of the derivative of the Hamiltonian with respect to λ_i (essentially, the local electrostatic potential), the imposed pH, and an empirical function $F(\lambda_i)$. The function $F(\lambda)$, which essentially accounts for the gas-phase acidity of a specific group, is considered to be characteristic of a given type of ionizable group (*e.g.* amine, carboxylic acid, *etc.*), and precalibrated based on multiple molecular-dynamics simulations of simple monofunctional organic compounds with experimentally known pK_a s.

In a first study [27], the method was described in detail and its application illustrated by a series of constant-pH MD simulations of small monofunctional amines. In particular, we investigated the influence of the relaxation time used in the weak-coupling scheme, the choice of appropriate model compounds for the calibration of the required empirical functions $F(\lambda)$, and corrections for finite-size effects linked with the small size of the simulation box. The method is currently being tested on small bifunctional compounds. As an illustration, the result of a constant-pH simulation of 1,4-butanediamine (putrescine; $pK_{a,1}^{exp}=9.22$, $pK_{a,2}^{exp}=10.69$) at $pH=1/2(pK_{a,1}^{exp} + pK_{a,2}^{exp})=9.96$ (1 ns) followed by a jump

to $pH=7$ and subsequent simulation (0.5 ns) are displayed in Fig. 2. At $pH=9.96$, the protonation states ($\lambda_1; \lambda_2$) progressively relax from the initial values of (0.5;0.5) to the expected values of (0.0;1.0). Simultaneously, the configuration adopted by the diamine progressively changes to allow for a hydrogen bond between the charged ammonium end and the neutral amino end, as observed experimentally. Upon lowering the pH to 7, the protonation states evolves towards (0.0;0.0) and the doubly-protonated diamine reverts to an extended conformation.

After calibration for other monofunctional organic compounds and further testing on small polyfunctional compounds, the method will be applied to the study of pH-dependent processes in peptides and proteins. Since the pH is an essential determinant of the structure (*e.g.* pH-induced denaturation, molten globules [24][25]) and function (*e.g.* substrate recognition, enzymatic catalysis) of biomolecules, constant-pH simulations will certainly find numerous useful applications in the study of biologically relevant problems. Ultimately, this new algorithm should become a routine tool in molecular simulations, just as are constant temperature and constant pressure algorithms [2][26].

Effect of Charged Residues on Protein Stability

Whether electrostatic interactions, and in particular the contribution of charged residues, have a significant influence on the stability of proteins is still a matter of debate [28]. Experimental mutational studies only provide an ambiguous answer to this question, because the mutation of a charged sidechain into a neutral one also involves, in addition to the electrostatic contribution, changes in van der Waals contacts, hydrogen-bonding patterns, and possibly conformational entropy. Thus, computational studies can be of great help in trying to isolate the different contributions to protein stability and understand, at the atomic level, the role of electrostatic interactions involving charged residues. Two examples of such studies from our work are discussed below, concerning (i) the effect of charge mutations on the stability of the enzyme staphylococcal nuclease, and (ii) the role of surface salt bridges on the stability of the hyperthermophilic protein Sac7d.

Staphylococcal nuclease is a small single-domain enzyme which has been extensively investigated by mutational

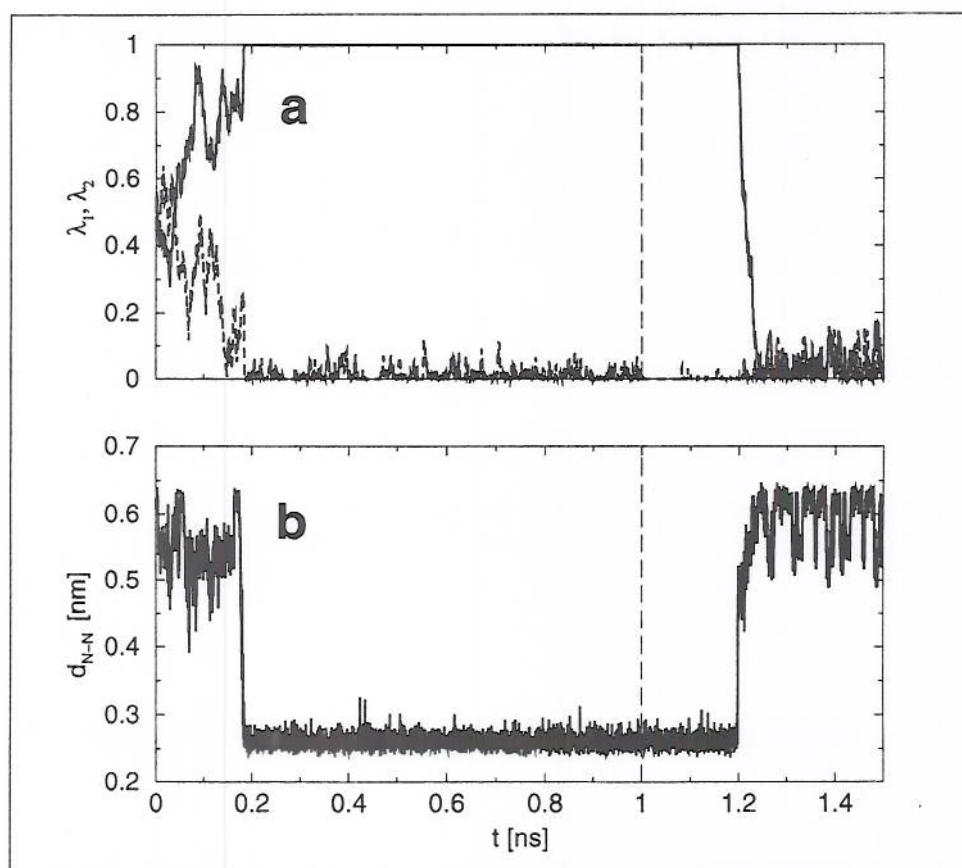


Fig. 2. Constant-pH simulation of 1,4-butanediamine (putrescine; $pK_{a,1}^{\text{exp}}=9.22$, $pK_{a,2}^{\text{exp}}=10.69$) using weak-coupling to a proton bath [27]: (a) extents of deprotonation λ_1 and λ_2 of the two amino groups (zero: fully protonated; one: fully deprotonated), and (b) distance d_{N-N} between the two nitrogen atoms. The simulation consists of 1 ns at $\text{pH}=1/2(pK_{a,1}^{\text{exp}} + pK_{a,2}^{\text{exp}})=9.96$ followed by 0.5 ns at $\text{pH}=7$. The extended (all-*trans*) configuration corresponds to $d_{N-N}=0.64$ nm, while configurations with $d_{N-N} \leq 0.3$ nm typically possess an intramolecular hydrogen bond.

studies [29][30]. In particular, the (guanidinium-induced) unfolding free energies $\Delta G_M^{\text{F} \rightarrow \text{U}}$ for the 48 single mutants involving the deletion of a charge (mutation to alanine) have been measured [30]. Comparing these to the corresponding value $\Delta G_W^{\text{F} \rightarrow \text{U}}$ for the wild type enzyme, one may express the relative stability of any charge mutant as $\Delta \Delta G_M^{\text{exp}} \equiv \Delta G_M^{\text{F} \rightarrow \text{U}} - \Delta G_W^{\text{F} \rightarrow \text{U}}$. Using an implicit solvation model (finite-difference solution of the Poisson equation [21] complemented by a surface-area-dependent non-polar term) and the experimental crystal structure of the enzyme, we estimated the free energy changes $\Delta G_{W \rightarrow M}^{\text{F}}$ caused by these 48 mutations in the folded state of the wild-type protein [31]. Assuming a linear relationship between these free-energy changes and those occurring in the unfolded state, namely $\Delta G_{W \rightarrow M}^{\text{U}} \approx \alpha \Delta G_{W \rightarrow M}^{\text{F}} + \beta$, one may compute a theoretical estimate for the relative stability of any charge mutant as $\Delta \Delta G_M^{\text{calc}} \equiv \Delta G_{W \rightarrow M}^{\text{U}} - \Delta G_{W \rightarrow M}^{\text{F}}$. Three parameters entering into the definition of the implicit-solvent model were treated as empirical, and optimized to yield the best corre-

lation between $\Delta \Delta G_M^{\text{exp}}$ and $\Delta \Delta G_M^{\text{calc}}$: the low dielectric permittivity corresponding to the protein interior, the proportionality factor between the surface area and the non-polar free-energy contribution, and a scaling factor applied to the atomic radii. The optimal choice resulted in the correlation between theory and experiment displayed in Fig. 3 (correlation coefficient of 0.83). The simple implicit-solvent model used in this study is able to predict relative changes in the stability of charge mutants almost within chemical accuracy: the root-mean-square deviation between experimental and calculated values is 2.9 kJ/mol (about $k_B T$). Indeed, values calculated for 14 other mutants in which a charged sidechain is mutated to a neutral one (differing from alanine and glycine) are in good agreement with the corresponding experimental values (see Fig. 3). Thus, calculations of this kind may be a valuable guide for the design of mutant enzymes with increased stability. Another consequence of the observed agreement is that assuming $\Delta G_{W \rightarrow M}^{\text{U}}$ to be linearly related with $\Delta G_{W \rightarrow M}^{\text{F}}$ appears to be reasonable.

Since, in addition, the slope of the correlation between these two quantities is close to one ($\alpha=0.93$), it appears that electrostatic interactions between charged residues in the unfolded state are surprisingly similar to those occurring in the native state. This result seems to indicate that, although dynamically disordered and lacking stable secondary structure, the unfolded state is far from random and quite similar to the folded state, at least in terms of the overall spatial distribution of charged residues.

The second example presented here questions the role played by salt bridges in the thermal stability of proteins. Hyperthermophilic organisms have the ability to grow under conditions of extreme temperatures (typically 80–100 °C; [32]). Understanding how the proteins involved in their metabolism can maintain their structure and activity under such elevated temperatures may provide valuable clues for a better understanding of protein folding and stability, and have important biotechnological applications. The DNA-binding protein Sac7d from *Sulfolobus acidocaldarius* is the smallest hyperthermophilic protein with available three-dimensional structure [33]. It is a 66-residue protein presenting as many as 32 ionized residues on its surface. An increased number of surface salt bridges is a common feature of hyperthermophilic proteins compared to their mesophilic homologues [32]. However, salt bridges are generally thought to be of minor importance in protein stability at room temperature [34]. To understand why this may no longer be true at elevated temperatures, we undertook two explicit-solvent simulations of this protein at 300K and 360K using the P³M [17] method to handle electrostatic interactions [35]. Both trajectories were shown to be stable on the nanosecond timescale. The simulations at 300 K and (to a lesser extent) 360 K were also in good agreement with NMR-derived distances. Raising the temperature from 300 K to 360 K resulted in a less favorable protein-solvent interaction energy, consequence of the increased thermal motion in the solvent, and a more favorable intraprotein interaction energy, essentially due to the tightening of salt bridges. Both effects were almost exclusively electrostatic in nature and dominated by contributions due to charged sidechains. This study showed that surface-charged residues are likely to contribute to protein stability at elevated temperatures because (i) the solvation free energy of charged sidechains is more adversely affected in the unfolded

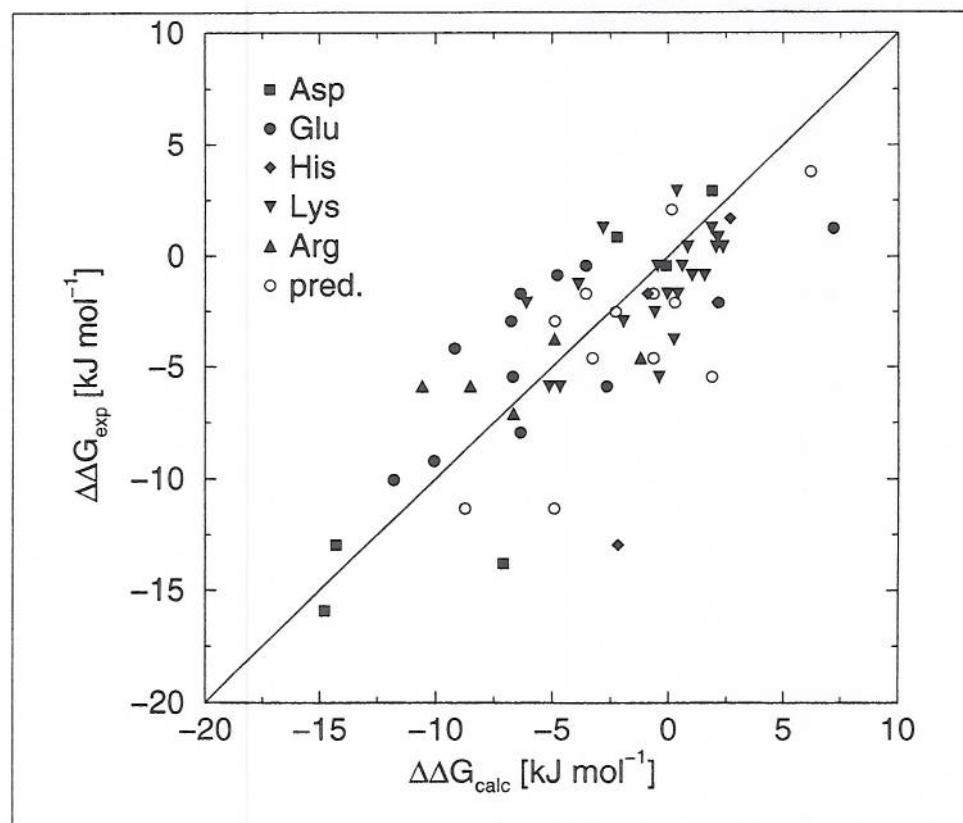


Fig. 3. Correlation between the experimental ($\Delta\Delta G_{\text{M}}^{\text{exp}} \equiv \Delta G_{\text{M}}^{\text{F}\rightarrow\text{U}} - \Delta G_{\text{W}}^{\text{F}\rightarrow\text{U}}$) and theoretical ($\Delta\Delta G_{\text{M}}^{\text{calc}} \equiv \Delta G_{\text{U}\rightarrow\text{M}}^{\text{U}} - \Delta G_{\text{W}\rightarrow\text{M}}^{\text{U}}$) relative stabilities of charge mutants of staphylococcal nuclease. Filled symbols represent 48 mutations (charged residue to alanine) based on which the three model parameters were optimized. Open circles represent 14 other mutants in which a charged sidechain is mutated to a neutral one (differing from alanine and glycine).

state than in the folded state by an increase in temperature, and (ii) due to the tightening of salt bridges, unfolding implies a larger unfavorable increase in the intraprotein Coulombic energy at higher temperatures.

Computer Simulation of Oligo- and Polysaccharides

In the past few years, the scientific community has shown a renewed interest for carbohydrates, driven in particular by their importance in biochemistry, industrial processes, and in the design of new materials [36]. However, the mechanisms responsible for the specific properties of many polysaccharide-based systems are still only partially understood. To investigate these mechanisms at the molecular level, computer simulation represents a powerful tool complementary to experiment. We are currently investigating three polysaccharide-based materials with specific interesting properties: (i) polyuronates, (ii) schizophyllan, and (iii) trehalose.

Polyuronates are linear polymers of uronic acids which can form gels in the

presence of divalent metal cations [36]. These polysaccharides have diverse biological functions in plants (preservation of the structure, texture, and prevention of desiccation) related to their ability to form gels. The most important natural derivatives of polyuronates are pectinates (and pectins) and alginates. The properties of natural polyuronate-based materials are largely used in the food industry (stabilizers, gelling, or emulsifying agents) and in the industries of cosmetics, textile, and paper. They also have many applications in the fields of medicine (encapsulation, prints), biochemistry (chromatography, culture media) and biotechnology (immobilization of enzymes). The four main building blocks of natural polyuronates are α -D-galacturonate, α -L-guluronate, β -D-mannuronate, and β -D-glucuronate, in a (1 \rightarrow 4) linkage. Concentrating on oligosaccharides based on these four components, we are currently investigating, using molecular dynamics simulations and continuum electrostatics calculations, the nature of the interactions in the gel phase, and the influence of different factors such as polysaccharide sequence, chain length, concentration, and type of cations, on gel formation.

Schizophyllan is a gel-forming glucan based on a tetrasaccharide unit [\rightarrow 3) Glc β (1 \rightarrow 3)Glc β (1 \rightarrow 3)Glc β (1] with a β (1 \rightarrow 6)Glc branch [37]. In solution and in the crystalline state, this polysaccharide adopts the structure of a triple helix, with the β (1 \rightarrow 6)Glc branches pointing towards the outside. Interestingly, two forms of the triple helix can be observed in aqueous solution, with a transition from form I to form II upon raising the temperature above 6 °C [38][39]. It has been suggested that this transition corresponds to an order-disorder transition. In this hypothesis, the β (1 \rightarrow 6)Glc branches are locked in helix I in rigid conformations through the bridging of two water molecules between successive branches along one strand, but become essentially free to rotate in helix II [38]. In order to examine this hypothesis, we have undertaken explicit-solvent simulations of a schizophyllan triple-helical segment at different temperatures.

Trehalose is a non-reducing disaccharide composed of two α (1 \rightarrow 1)-linked glucopyranose residues. This compound is present in large amounts in certain plants of the desert and in some animals such as tardigrades and the brine shrimp *Artemia salina* capable of surviving almost complete dehydration at elevated temperatures [40]. Although the biological function of these organisms is interrupted under these conditions, trehalose stabilizes biological structures in the dehydrated form and restores them intact and functional as soon as the hydration and temperature conditions are more favorable, a phenomenon known as cryptobiosis. In other freeze-tolerant organisms, trehalose plays a similar role as a cryoprotectant. Trehalose or other polysaccharide-based materials with similar properties have many potential scientific and industrial applications e.g. (i) the preservation of delicate biological structures (proteins, living cells) at ambient temperature (alternative to lyophilisation); (ii) the use of trehalose-based glasses for crystallogenesis of proteins and membrane-based systems; (iii) the coating of dried food so as to preserve it from degradation and to prevent liposoluble compounds (flavors) to escape; (iv) the stabilization (and even activation) of thermolabile enzymes at elevated temperatures.

Although many hypotheses have been formulated, the mechanism by which trehalose stabilizes the structure of proteins and membranes under conditions of temperature and hygroscopy that would normally promote their denaturation is

still unknown. The two main hypotheses involve either the direct interaction (through hydrogen bonds) between trehalose and the protected structure [40][41], or the trapping of water close to the biomolecular surface [42]. Using molecular dynamics simulations we are trying to understand the physico-chemical properties and mechanism of action of the trehalose molecule. To this purpose, several simulations of pure trehalose in water at different concentrations, of a protein (lysozyme) in a concentrated trehalose solution, and of a membrane patch (dipalmitoyl-phosphatidylcholine) surrounded by a trehalose solution have been undertaken. Preliminary results on the lysozyme/trehalose system indicate that the trehalose tends to replace some of the water molecules at the protein surface, and to interact directly with the protein through hydrogen bonds (see Fig. 4).

Received: June 16, 2001

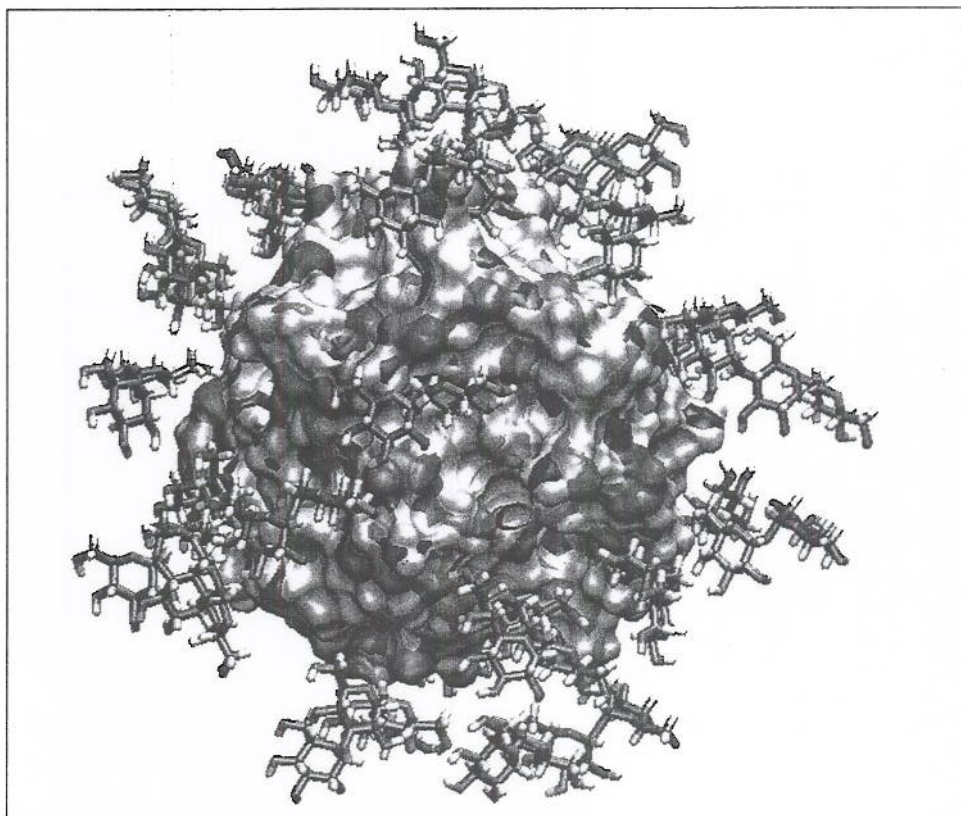


Fig.4. Lysozyme coated by trehalose molecules. This conformation is issued from a 100 ps molecular dynamics simulation at 298 K of a system containing one lysozyme molecule, 32 trehalose molecules, 8 Cl⁻ ions and 9966 water molecules. The molecular surface of the protein is represented, color coded according to atom type (C: cyan; O: red; H: white; N: blue). Trehalose molecules are displayed using sticks (C: gray; O: red; H: white). Water molecules were removed for clarity. Within the short (100 ps) simulation period, the number of hydrogen-bonds between trehalose molecules and the protein has increased by about a factor of two.

- [1] P.H. Hünenberger, W.F. van Gunsteren, in 'Computer simulation of biomolecular systems, theoretical and experimental applications', Vol. 3, Eds. W.F. van Gunsteren, P.K. Weiner, A.J. Wilkinson, Kluwer/Escom Science Publishers, Dordrecht, The Netherlands, **1997**, p. 3.
- [2] W.F. van Gunsteren, H.J.C. Berendsen, *Angew. Chem. Int. Ed. Engl.* **1990**, *29*, 992.
- [3] P.E. Smith, W.F. van Gunsteren, in 'Computer simulation of biomolecular systems, theoretical and experimental applications', Vol. 2, Eds. W.F. van Gunsteren, P.K. Weiner, A.J. Wilkinson, ESCOM Science Publishers, B.V., Leiden, The Netherlands, **1993**, p. 182.
- [4] R.M. Levy, E. Gallicchio, *Annu. Rev. Phys. Chem.* **1998**, *49*, 531.
- [5] P.H. Hünenberger, in 'Simulation and theory of electrostatic interactions in solution: Computational chemistry, biophysics, and aqueous solution', Eds. G. Hummer, L.R. Pratt, American Institute of Physics, New York, U.S.A., **1999**, p. 17.
- [6] M.P. Allen, D.J. Tildesley, 'Computer simulation of liquids', Oxford University Press, New York, **1987**.
- [7] M. Neumann, O. Steinhauser, G.S. Pawley, *Mol. Phys.* **1984**, *52*, 97.
- [8] T.P. Straatsma, H.J.C. Berendsen, *J. Chem. Phys.* **1989**, *89*, 5876.
- [9] H. Schreiber, O. Steinhauser, *Chem. Phys.* **1992**, *168*, 75.
- [10] G. Hummer, D.M. Soumpasis, M. Neumann, *Mol. Phys.* **1993**, *81*, 1155.
- [11] R.H. Wood, *J. Chem. Phys.* **1995**, *103*, 6177.
- [12] N.A. Baker, P.H. Hünenberger, J.A. McCammon, *J. Chem. Phys.* **1999**, *110*, 10679.
- [13] P.H. Hünenberger, J.A. McCammon, *J. Chem. Phys.* **1999**, *110*, 1856.
- [14] J.A. Barker, R.O. Watts, *Mol. Phys.* **1973**, *26*, 789.
- [15] I.G. Tironi, R. Sperb, P.E. Smith, W.F. van Gunsteren, *J. Chem. Phys.* **1995**, *102*, 545.
- [16] P.P. Ewald, *Ann. Phys.* **1921**, *64*, 253.
- [17] R.W. Hockney, J.W. Eastwood, 'Computer simulation using particles', Institute of Physics Publishing, Bristol, **1981**.
- [18] U. Essmann, L. Perera, M.L. Berkowitz, T. Darden, H. Lee, L.G. Pedersen, *J. Chem. Phys.* **1995**, *103*, 8577.
- [19] P.H. Hünenberger, J.A. McCammon, *Biophys. Chem.* **1999**, *78*, 69.
- [20] W. Weber, P.H. Hünenberger, J.A. McCammon, *J. Phys. Chem. B* **2000**, *104*, 3668.
- [21] J.D. Madura, M.E. Davis, M.K. Gilson, R.C. Wade, B.A. Luty, J.A. McCammon, in 'Reviews in computational chemistry', Vol 4, Eds K.B. Lipkowitz, D.B. Boyd, VCH Publishers, Inc., New York, **1994**, p. 229.
- [22] C. Peter, W.F. van Gunsteren, P.H. Hünenberger, to be submitted.
- [23] S. Sasso, P.H. Hünenberger, to be submitted.
- [24] T.E. Creighton, *Biochem. J.* **1990**, *270*, 1.
- [25] H. Christensen, R.H. Pain, *Eur. Biophys. J.* **1991**, *19*, 221.
- [26] H.J.C. Berendsen, J.P.M. Postma, W.F. van Gunsteren, A. DiNola, J.R. Haak, *J. Chem. Phys.* **1984**, *81*, 3684.
- [27] U. Börjesson, P.H. Hünenberger, *J. Chem. Phys.* **2001**, *114*, 9706.
- [28] B. Honig, A.-S. Yang, *Adv. Prot. Chem.* **1995**, *46*, 27.
- [29] D. Shortle, *Adv. Prot. Chem.* **1995**, *46*, 217.
- [30] A.K. Meeker, B. Garcia-Moreno, D. Shortle, *Biochemistry.* **1996**, *35*, 6443.
- [31] U. Börjesson, P.H. Hünenberger, to be submitted.
- [32] M.T. Madigan, B.L. Marrs, *Sci. Am.* **1997**, *276*, 66.
- [33] S.P. Edmondson, L. Qiu, J.W. Shriver, *Biochemistry* **1995**, *34*, 13289.
- [34] Z.S. Hendsch, B. Tidor, *Protein Sci.* **1994**, *3*, 211.
- [35] P.I.W. de Bakker, P.H. Hünenberger, J.A. McCammon, *J. Mol. Biol.* **1999**, *285*, 1811.
- [36] J.F. Robyt, 'Essentials of carbohydrate chemistry', Springer Verlag, New York, **1998**.
- [37] T. N. McIntire, A. Brant, *J. Am. Chem. Soc.* **1998**, *120*, 6909.
- [38] T. Itou, A. Teramoto, T. Matsuo, H. Suga, *Carbohydrate Res.* **1987**, *160*, 243.
- [39] A. Teramoto, H. Gu, Y. Miyazaki, M. Sorai, S. Mashimo, *Biopolymers* **1995**, *36*, 803.
- [40] J.H. Crowe, J.F. Carpenter, L.M. Crowe, *Annu. Rev. Physiol.* **1998**, *60*, 73.
- [41] S.D. Allison, B. Chang, T.W. Randolph, J.F. Carpenter, *Arch. Biochem. Biophys.* **1999**, *365*, 289.
- [42] P.S. Belton, A.M. Gil, *Biopolymers* **1994**, *34*, 957.